Title
STRESSED MIRROR POLISHING: FABRICATION OF AN OFF-AXIS SECTION OF A PARABOLOID

Author
Nelson, J.E.

Publication Date
1979-12-01

Lawrence Berkeley Laboratory
UNIVERSITY OF CALIFORNIA

Physics, Computer Science & Mathematics Division

Submitted to Applied Optics

STRESSED MIRROR POLISHING: FABRICATION OF AN OFF-AXIS SECTION OF A PARABOLOID

Jerry E. Nelson, George Gabor, Leslie K. Hunt, Jacob Lubliner, and Terry S. Mast

December 1979

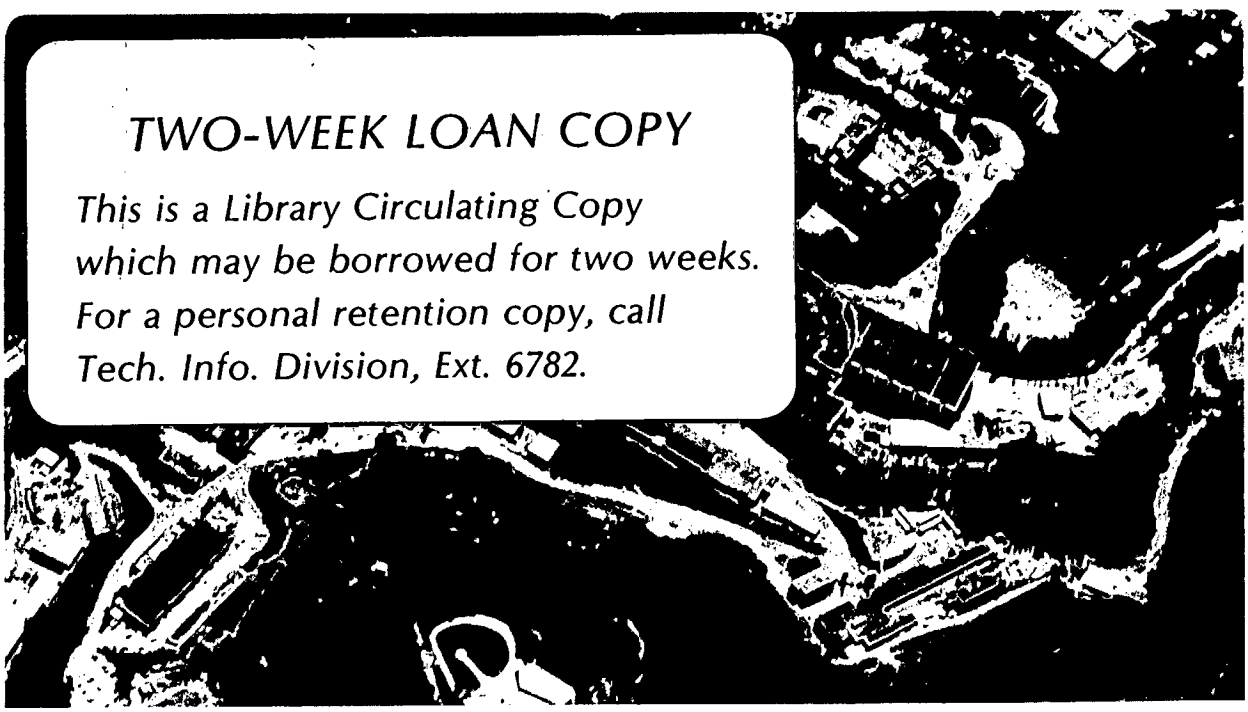

Prepared for the U.S. Department of Energy under Contract W-7405-ENG-48

DISCLAIMER

LBL#9968

Stressed Mirror Polishing: Fabrication of an Off-Axis Section of a Paraboloid

Jerry E. Nelson, George Gabor, Leslie K. Hunt,
Jacob Lubliner, and Terry S. Mast

Lawrence Berkeley Laboratory and University of California, Berkeley

ABSTRACT

We have fabricated a mirror with the shape of an off-axis section of a paraboloid by grinding and polishing a sphere into a prestressed blank. The applied stresses were then removed allowing the mirror to spring into the desired paraboloidal shape. The 36 cm diameter off-axis section deviated 9.9 μm rms from the polished sphere. The final surface deviated 0.03 μm rms from the desired off-axis section.

Stressed Mirror Polishing: Fabrication of an Off-Axis Section of a Paraboloid

Jerry E. Nelson, George Gabor, Leslie K. Hunt,
Jacob Lubliner, and Terry S. Mast

Lawrence Berkeley Laboratory and University of California, Berkeley

I. Introduction

A new technique for fabricating mirrors with non-axisymmetric surfaces is described in an adjoining article by Lubliner and Nelson[1] (hereafter LN). In this paper we report the use of that technique to fabricate an off-axis section of a paraboloid. The theoretical basis of the technique was developed, and this experiment was carried out, to demonstrate the feasibility of economically producing a matched set of off-axis segments, capable of being assembled into a much larger mirror. This is one of the designs being considered for a proposed University of California Ten-Meter Telescope[2]. The design calls for a primary mirror composed of 60 hexagonal segments, each 1.4 m in diameter and 10 cm thick[3, 4, 5].

The parameters of the mirror for this demonstration were selected in order to test the technique in general, and to demonstrate its applicability to making the Ten-Meter Telescope mirror segments. As a matter of economy, a quarter scale mirror was selected, about 36 cm in diameter. The diameter-to-thickness ratio was set at 14 to 1, the same as that needed for the 1.4 m segments.

To make the off-axis section we deliberately deform a mirror blank prior to and during grinding and polishing. This is carried out by applying a uniform pressure across the back of the blank and applying shear forces and torques around its circumference. The purpose is to deform the blank such that after a sphere is polished into it and the applied forces are removed, the mirror will spring into the desired shape. LN describe the method for finding the necessary forces to bend an off-axis section of a paraboloid (or any of a large class of surfaces) into a sphere. The method assumes the mirror is of uniform thickness and that the sagittal depth is small compared to the mirror thickness. Since the basis of the method is to strain the blank elastically, the technique is limited to those cases where the necessary stress is below the elastic limit for the material, or for glass, below the breaking stress. Thus very thick mirrors that are extremely aspheric may not be good candidates for this method.

In Section 2 we describe the geometry of the mirror, giving the equation of the desired surface. Since we wished to demonstrate the applicability of this technique to making a matched set of mirrors, we sought to make a segment with an accurately specified radius of curvature and off-axis distance. The method of stressing the blank is explained in Section 3. A relatively simple jig using weights and levers is used to apply torques and shear forces at 24 places around the circumference. The compression of a rubber pad beneath the blank provides a uniform pressure to the back. Section 4 describes the grinding, polishing, and testing procedures. Approximations and errors in the procedure necessitate iterations of the polishing and testing cycle. The rate of convergence was such that after two polishings the rms

surface deviation from the desired surface was 0.03 μm. In the final section we discuss the results of this demonstration and the technique in general. A number of "measures of difficulty" of producing various non-axisymmetric surfaces are presented. These are then used to assess the validity of extrapolating the results of this demonstration to the production of larger segments.

II. The Mirror Shape

The mirror blank was a piece of premium quality low thermal expansion glass (CerVit by Owens-Illinois) 35.88 cm in diameter and 2.54 cm thick. The blank was of constant thickness, as needed for the method under test. The top surface was ground concave to an approximate radius of 374 cm and the back surface was ground and polished convex to a radius of 377 cm.

In general, one can write the equation for the surface shape of an off-axis paraboloid section in local coordinates (defined in Figure 1) as

$$z(\rho,\theta) = \alpha_{20}\,\rho^2 + \alpha_{22}\,\rho^2\cos2\theta + \alpha_{31}\,\rho^3\cos\theta + \alpha_{33}\,\rho^3\cos3\theta + \alpha_{40}\,\rho^4 + \alpha_{42}\,\rho^4\cos2\theta \qquad (2.1)$$

where the higher order terms are usually negligible. Defining the off-axis distance to the center of the segment as R, the paraboloid radius of curvature by k, the segment radius by a, $\epsilon = R/k$, and $\rho = r/a$ one can show (see LN) that

$$\alpha_{20} = \frac{a^2}{2k}\left(1 - \epsilon^2 + \frac{9}{8}\epsilon^4 - \frac{5}{4}\epsilon^6 + \dots\right) \qquad \text{(focus)}$$

$$\alpha_{22} = -\frac{a^2R^2}{4k^3}\left(1 - \frac{3}{2}\epsilon^2 + \frac{15}{8}\epsilon^4 + \dots\right) \qquad \text{(astigmatism)}$$

$$\alpha_{31} = -\frac{a^3R}{2k^3}\left(1 - \frac{11}{4}\epsilon^2 + \frac{21}{4}\epsilon^4 + \dots\right) \qquad \text{(coma)}$$

$$\alpha_{33} = \frac{a^3R^3}{8k^5}\left(1 - 3\epsilon^2 + 6\epsilon^4 + \dots\right) \qquad (2.2)$$

$$\alpha_{40} = \frac{3a^4R^2}{8k^5}\left(1 - 4\epsilon^2 + \frac{41}{4}\epsilon^4 + \dots\right) \qquad \text{(spherical aberration)}$$

$$\alpha_{42} = \frac{a^4R^2}{4k^5}\left(1 - 5\epsilon^2 + \frac{115}{8}\epsilon^4 + \dots\right)$$

Similarly, a sphere of radius ℓ can be described by

$$z(\rho,\theta) = \frac{a^2}{2\ell}\rho^2 + \frac{a^4}{8\ell^3}\rho^4 + \frac{a^6}{16\ell^5}\rho^6 + \ldots \qquad (2.3)$$

If this is the sphere which is polished into the blank, then the desired deflection imposed by the stressing jig is given by the difference of (2.3) and (2.1). The sphere radius can in principle have any value; however, two values are of particular interest. The sphere can be chosen to create the smallest rms deflections in the surface or alternatively, the sphere can be chosen to minimize maximum stress in the blank. These two spheres are slightly different and lead to rms deflections and maximum stress differences typically of order 20%. For our test piece we chose a configuration which was close to the lowest stress configuration and which also gave large deflections. Using the formula of LN, we selected k = 368.80 cm, R = 35.0 cm and ℓ = 373.80 cm. (Initially, we selected ℓ = 373.87 cm as that was the nominal radius of curvature of the reference sphere used for testing during polishing. We later discovered that the reference sphere actually used had ℓ = 373.80 cm. This discrepancy only affects the radius of curvature of the parabola achieved in the first polish. It has no effect on the surfaces achieved in subsequent polishes or the final paraboloidal surface.)

For convenience we chose to describe the surface deflections with the orthogonal set of functions called Zernike polynomials, $Z_{nm}(\rho,\theta)$. Thus the surface and desired deflections can be written in the form

$$z(\rho,\theta) = \sum_{n=0}^{\infty} \sum_{m=-n}^{n} C_{nm} Z_{nm}(\rho,\theta) \qquad n-m \text{ even} \qquad (2.4)$$

The polynomials are defined in Table 1. Also listed are the Zernike coefficients for the desired off-axis section and the desired deflection for the test piece (the difference between (2.3) and (2.1)). The relationship between Zernike coefficients C_{nm} and the polynomial coefficients, α_{ij} used above is given in column 4 of Table 1. The orthogonality of the Zernike polynomials implies a simple relation between the coefficients of a surface and the rms amplitude, σ, averaged over the surface:

$$\sigma = \left[\sum_{n=0}^{\infty} \sum_{m=-n}^{n} w_{nm} C_{nm} \right]^{\frac{1}{2}} \quad \text{where} \quad w_{nm} = \frac{1 + \delta_{m,0}}{2(n + 1)} \qquad (2.5)$$

and $\delta_{m,0}$ is the Kronecker delta. The size of the individual terms in the deflection are shown as a function of off-axis distance, R, in Figure 2. Also plotted is the rms surface deflection as a function of R. The non-axisymmetric surface terms of the surface expansion of the demonstration piece (R = 35 cm) are dominated by the astigmatic and comatic terms. The rms surface deflection is 9.9 μm. Thus the grinding and polishing procedure involves the removal of about 10 μm of material.

III. Stressing the Mirror

Having established the parameters of the desired off-axis section and the sphere to be ground and polished into the blank (in this case defined by minimizing the maximum stress), the difference between equations 2.1 and 2.3 defines the required deflections. If these deflections are successfully imposed, then after the sphere has been polished and the externally applied forces are removed, the mirror will take the desired off-axis paraboloidal shape. This will only be true if the glass is elastic, i.e. does not undergo any plastic flow. Many glasses are almost ideal in this respect right up to the breaking point.

Since the act of grinding and polishing does of course change the thickness, the deflections which result from a given set of applied forces change as the material is removed. In practice these changes are very small and predictable in any case. In addition, changes in the internal stress of the blank may result from grinding and polishing with consequent deformations. However, this effect is the same as that encountered during the fabrication of any optical component, and the resulting deformations are automatically eliminated by the optician during grinding and polishing. Internal stresses do not affect the deflections induced by the applied forces since glass behaves in a linear fashion (stress is proportional to strain).

The deformations required for most mirrors are of low order, 4th order or less. It is possible to achieve these low order deformations by applying forces and couples only around the edge of the blank along with uniform pressure on back (see LN). In practice it is convenient to apply the edge forces at discrete points rather than continuously and

for this demonstration we chose 24 equally spaced points. Since the highest angular term of interest is cos(3θ), 24 points are more than adequate. Angular terms up to and including cos(12θ) can be controlled with 24 points, so the effects of discreteness in applying the necessary forces and couples produce only high angular frequency errors. Since, mathematically, the radial function must be at least as high an order as the angular one, the lowest order surface error caused by discreteness will be of the form $Z_{13,13} = \rho^{13}\cos(13\theta)$ and $Z_{-13,13} = \rho^{13}\sin(13\theta)$. When these terms appear in the mirror, they only affect the outer edge. Over the bulk of the mirror surface, the high order terms make a negligible contribution. As described below in section 4, high-spatial-frequency edge effects do occur. These could be reduced by applying forces and couples at more points. Alternatively, the blank can be made slightly larger than the final desired mirror to allow for removal of the outer edge after polishing.

Couples and forces were applied through 24 Invar blocks bonded to the edge of the blank with epoxy . The blocks were 2.2 cm high, 4.4 cm wide and 1.7 cm thick and shaped on the inner side to match the curvature of the blank. Invar, a low thermal expansion steel, was used to minimize thermal stresses imposed on the blank by the blocks. Since the applied stresses were expected to reach 70 kg/cm^2 (1000 psi), tests were made to ensure that the bonding was secure. It is also important that the bonding be as stress-free as possible, since the blocks need to be removed after polishing without warping the mirror. We tested a number of adhesives and various techniques of applying the blocks in a stress-free fashion. For the method finally chosen, we etched the glass surface with hydrofluoric acid, cleaned it, and using Emerson-Cummins

2850FT epoxy, bonded the Invar to the glass. The bond was approximately 0.2 mm thick and the blocks were held without compression against the mirror during curing. Even with this technique, stress patterns in the glass were observed using crossed polaroids. We assume these were caused by epoxy shrinkage during curing. However interferometric tests of a mirror before and after attaching the 24 blocks revealed no measurable change in the surface. (If the maximum required stress is lower than 70 kg/cm^2, RTV adhesives would probably work and greatly reduce the stress induced in the blank.) With the above procedures, the bonds were tested and typically failed at induced stress levels of 200 kg/cm^2 where the failure was in the glass, not in the bond.

The necessary forces and couples to be applied through the blocks were calculated from the formulas given by LN. These included forces and couples for a variety of axisymmetric and non-axisymmetric tests which were performed, as well as those for the desired off-axis section of a paraboloid.

A radial arm 30 cm long was bolted onto each block. Using a system of lead weights, levers, and fulcra, a pair of forces of adjustable sign and amplitude were applied to each of the 24 radial arms in order to achieve the desired force and couple at the edge of the blank. Figure 3 is a schematic of the lever system. An arbitrary force and couple can be supplied by the appropriate values of F_1 and F_2 applied with arm lengths r_1 and r_2. Bearings were located at all pivot points, the weights were calibrated to ± 1 gram and friction in the system was minimized. The design of the jig was such that the applied forces and couples were unaffected by small displacements of the mirror. This is critical,

since the mirror may move vertically during polishing. We estimate the applied forces and couples were accurate to about 0.1%.

Since the stressing jig rotated on the polishing table, bearing stops were also used to limit the radial motion of the weights. To limit any radial motion of the blank caused by tool loads during grinding and polishing, four of the 24 radial arms were equipped with radial thrust bars, which effectively prohibited radial motion without introducing any undesirable vertical forces.

The blank is pressed downwards by the net shear force imposed by the radial arms as well as by the grinding and polishing tool loads. To accommodate this load, we placed the blank on a soft pad which in turn rested on a stiff (5 cm thick) steel plate with a surface machined concave to the same radius of curvature as the mirror's. The plate was a rigid part of the entire jig and acted as a base against which displacements were measured and forces applied.

Only one of the desired deflection terms, C_{40}, containing a deformation, $\sim p^4$, requires the use of the pad. The value of C_{40} is 0.40 μm. To achieve this deflection we require that the pad push uniformly upwards over the entire back surface of the blank. Stated another way, uniform pressure on the back of the blank produces a quadratic and quartic deflection.

The seemingly simple requirement that a pad provide a sufficiently uniform pressure proved to be the single most troublesome part of the mirror bending procedure. The average value of the pressure is set by the conditions of static equilibrium; the integrated pad pressure

exactly balances the net downwards force applied by the arms plus the weight of the blank itself. This net force is, by design, that needed to introduce the necessary quartic. However, small deviations from uniformity in the pad can cause unwanted deflections. A theoretical relationship between the amplitude of the unwanted deflections and the deviations from pad uniformity is given in Appendix 1. The most readily induced deflection is astigmatism, and its amplitude is over 10 times the fractional (astigmatic) non-uniformity in the pad multiplied by the desired quartic. Thus a 1% astigmatic term in the pad will produce 0.05 μm of astigmatism in the mirror.

For this demonstration, we chose to deal empirically with the problems introduced by a non-uniform pad. We experimented with several pad types, both fluid and elastic. In principle fluid pads should give a completely uniform support, but two practical problems limit their usefulness: difficulty in obtaining uniform pressure out to the very edge of the blank, and instability against small turning moments. Tests with a self-contained fluid pad, a thin vinyl bag of water, showed the same level of unwanted deflections as other pads, presumably due to improper support at the edge. The problem of stability was even more serious, since the lack of restoring forces to turning moments caused the blank to rock.

Elastic pads have several important advantages. They can be made simply and economically. They naturally balance any small turning moments and are thus stable, and because of this characteristic (see LN), they allow complete control over all 5th order surfaces, instead of 4th order, as for fluid pads. We sought a pad which compressed a dis-

tance much greater than the mirror deformation so that the mirror deflections themselves would not appreciably alter the pressure distribution of the pad. For our test mirror, the peak to peak deflections are 60 μm, so a pad compression of about 1 mm was chosen.

The elastic pads tested were open and closed cell neoprene and natural rubber of various types. Tests were performed by pulling down uniformly around the edge of a spherical mirror to produce the desired quartic term. Then the mirror was examined interferometrically with a spherical null test to look for non-axisymmetric deflections. The positions of the interference fringes were digitized and fit with Zernike polynomials so a quantitative measure of pad behavior was obtained. As expected from the analysis in Appendix 1, the dominant error was astigmatism. After testing continuous sheets, segmented pads, laminated and cross laminated pads, we selected a 3-ply cross laminated pad, 1 cm thick, that was composed of open cell natural rubber. This typically gave an astigmatic term $C_{22} \simeq 0.15$ μm with $C_{40} \simeq 0.50$ μm.

Deflections through 5th order caused by nonuniformities in the pad are in principle removable with the appropriate shear force and couple along the blank edge. In practice, the stability of these terms was troublesome, and forced us into a specific test cycle to be described later; we found that taking the mirror in and out of the jig could substantially alter non- axisymmetric deflections caused by the pad. We reduced this somewhat by placing a thin sheet of mylar between the blank and the pad, and once the pad was located on the steel plate, we avoided moving it.

To further test the jig, and the validity of the calculations, we

deformed a spherical mirror into a variety of shapes. Each deformed surface was tested with a Twyman-Green interferometer located at the center of curvature which provided a spherical null test. The fringe positions on the interferograms were digitized, fitted to Zernike polynomials, and the resulting coefficients were compared with those expected. By and large, we found agreement with our theoretical expectations to within 1 - 2%. Since some of the deformations made the mirror decidedly non-spherical, the interference fringe pattern became quite complex. Figure 5 shows the mirror warped into an off-axis "antiparaboloid" (the same magnitude deviation from a sphere as a paraboloid, but of opposite sign) and tested as a sphere; the Zernike coefficients from the fit to the measured fringe positions were used to generate the adjacent contour plot of the mirror surface. The saddle is due to the astigmatic term and the interior extremum is produced by the comatic term. The measurement uncertainties for these complex fringe patterns corresponded to surface uncertainties of 0.05 μm rms. When the fringe patterns were less complex the measurement and fitting uncertainties were much smaller.

The above series of tests provided us with several important conclusions: (1) the theoretical predictions were correct to within 2%, (2) the jig was capable of applying the forces and couples with a reproducibility of about 0.1%, (3) the jig was stable when subjected to shocks and vibrations as might occur during polishing, (4) a pad of sufficiently high quality could be made, if iterative testing and polishing is used. These results provide the necessary basis for using the stressing technique.

IV. Mirror Fabrication: Polishing, Testing, Iteration

The grinding and polishing procedures described here were carried out using standard commercial techniques at Tinsley Laboratories. The testing was done in consultation with the opticians at Tinsley.

A second blank of CerVit was prepared to be identical with the first one, except that the front surface was ground spherical, but not polished. The first mirror was not used since we felt it might be useful to have available a good spherical mirror in case further tests of the jig proved necessary. The second blank was placed in the jig and the weights were applied to impose the desired forces and couples calculated using the formulas of LN (see Table 2). These would distort a sphere into an off-axis antiparaboloid (or a paraboloid into a sphere). The ground surface then deviated from a sphere by about 60 μm peak-to-peak, with the largest contribution from astigmatism and coma.

A grinding tool the size of the blank was made with hexagonal ceramic tiles attached to an iron plate. The tool had approximately the desired radius of curvature ℓ = 373.87 cm. The optician began with 30 micron grit and worked the tool by hand into the blank for a few minutes, then allowed the arm of the polishing machine to provide the motive power. The grinding process continued using 30 micron, 12 micron, and finally 3 micron grits. The entire grinding procedure required about 7 hours.

Since the desired sphere had a specific radius, the surface was frequently tested with a spherometer during the grinding phase. The test consisted of comparing the sagittal depth of the blank against that

of a 20 cm diameter reference mirror. The difference in sagittal depths of the reference and ground surfaces was estimated at 0.5 μm (over the 20 cm diameter of the reference sphere) after the final grinding.

The reference mirror was purported to have a radius of curvature of 373.87 cm; this value was used in all calculations to establish the forces and couples. As mentioned earlier, the actual radius of the reference mirror was subsequently found to be 373.80 cm. This discrepancy was discovered by finding that after the first polish, the radius of curvature was unexpectedly short. The correct radius of the 20 cm reference mirror was then established by measuring the surface with a device at Tinsley Laboratories which employs a fringe counting interferometer.

In order to guarantee that the polished sphere have a reproducible radius of curvature, we decided to use the convex half of a matched pair of 20 cm test plates to test the polished surface. The concave part was used during grinding. Although the test plate was undersized (20 cm instead of 36 cm), and thus less accurate than a full sized one, the convenience and economy of this test method made it a reasonable solution to the problem of testing while polishing. In the hands of an experienced optician, this testing procedure allows one to distinguish surface differences caused by differences in radius of curvature, astigmatism, coma, etc., down to levels $< \sim \lambda/10$ rms ($\lambda = 0.6328\ \mu$).

After grinding, we proceeded with the polishing process. This was done in a conventional fashion with the jig on a rotating table, and the full sized polishing lap placed on the mirror surface; the lap was driven by a spindle both rotationally and radially. The polishing and

grinding machine is a Tinsley modification of the standard arc-type polishing machine with a 180 cm blank capacity. Polishing continued for about 25 hours at which point the surface differed from the test plate by about $\lambda/4$ rms, caused largely by a depression in the center of the mirror. Since we expected to make corrections and then polish a second time, a high quality sphere was not sought at this time. The weights were then removed from the jig, the radial arms detached from the invar blocks, and the mirror was removed for testing.

The test configuration shown in Figure 4 is a folded parabolic null test with the flat mirror folding the focal point back onto the vertex. Because we wanted a specific off-axis parabola, and expected multiple polish-test cycles, the mirror support was designed and tested to ensure the mirror could be located accurately and repeatedly with respect to the interferometer focus. By folding the focal point onto the vertex, the laser can be autocollimated by adjusting the tilt and displacement of the flat. The resulting perpendicular distance from the vertex to the flat is k/4 where k is the radius of curvature of the paraboloid.

Since the mirror was relatively thin and flexible it was simplest to support it on edge, rather than on its back. The mirror was held in a mount with micrometer control of three rotations and three translations and was attached to the mounting plate with a kinematic mount. Three V-blocks were fixed to the mounting plate: two oriented azimuthally and one radially. Three corresponding fixtures with spherical balls (1.27 cm diameter) were bolted onto three of the Invar blocks. The three balls fit into the V-blocks to just define the mirror position relative to the base plate.

The center and orientation of the mirror were defined by a stretched wire pattern. A 0.3 mm wire was strung across a set of four binding posts attached to the Invar blocks. This pattern was used to define the coordinates in the test interferograms and also in the surveying procedure which fixed the mirror position with respect to the vertex. The wire layout can be seen in Figures 6, 7, and 8 which show interferograms of the mirror.

The desired vertex location relative to the mirror was established by surveying. The location of the vertex along the optical axis (z coordinate) was set using a rod which pivoted about the center of curvature and had a dial indicator attached to its free end. The rod length was approximately the radius of curvature. By measuring the relative distances to various parts of the mirror surface, the desired relative distance to the vertex was established and a point attached to an xyz stage (in turn firmly attached to the mirror base plate) was adjusted to be at this distance. The other two coordinates of the vertex were set by placing a transit at the center of curvature and measuring the desired angle from the center (defined by the crossed wires) along one of the wires. These two coordinates (x,y) were established with an accuracy of 0.2 mm while the position along the optical axis (z) was set to an accuracy of .05 mm. The desired vertex point was defined by the intersection of two scribed lines on the surface of a plug which fit into a hole in a plate on the xyz stage. By design this point was coincident with the center of a 2.54 cm steel ball when the ball was placed against the hole (after removing the plug).

The Twyman-Green interferometer focus was located at the vertex by

placing the 2.54 cm polished steel ball against the hole on the xyz stage and autocollimating the interferometer on the ball surface. This accurately located the interferometer focal point at the center of the ball.

The ball was then removed and the wavefront allowed to pass through the optical system as shown in Figure 4. The returning focus was superimposed on the vertex (i.e. autocollimated) by tilting and translating the flat. The interferogram which results from this alignment process represents the difference between the optical surface under test and a parabolic surface whose off-axis distance is set by the surveying and whose radius of curvature is defined by the distance between the vertex and the flat, k/4.

This latter distance was measured using a rod with a 2.54 cm diameter ball attached to one end and a dial indicator attached to the other. The length was calibrated against a steel rule. The ball was placed against the hole on the xyz stage and the indicator end placed against the flat. The minimum distance measured established the perpendicular distance from the flat to the vertex, k/4; this distance was measured with an accuracy of 0.05 mm.

An interferogram taken after the first polish is shown in Figure 6. The positions of interferogram fringes were digitized, then were fitted to Zernike polynomials through 4th order, after the outer 5% of the radius had been masked off. The rms residual between the 4th order fit and the 450 digitized points was 0.02 μm, which indicates a good fit. The combination of these coefficients and the measurement of k/4 provides a complete description of the surface. The Zernike coefficients

describing the surface are listed in Table 1.

After the first polish the mirror had an rms deviation of 0.55 μm from the desired paraboloid. The largest error in the surface was due to the difference between the desired and achieved radii of curvatures. As mentioned earlier, this was traced to a mistaken radius of curvature attributed to the test plate. The imperfection of the spherical polish also contributed to the errors in the mirror.

After testing the mirror as a paraboloid the mirror was placed in the jig and the original forces and couples reapplied. This surface was tested as a sphere and the positions of the resulting interferogram fringes were digitized and fit to Zernike polynomials, as before. A complete description of the surface is given by these coefficients and the radius of curvature of the sphere which was assumed to be that of the test plate. This is a questionable assumption since the stated difficulties with the pad may have produced some change of radius when the mirror was placed in the jig. However, because of the inconvenience of measuring the radius directly, we chose to assume it had not changed.

The difference between the paraboloidal and spherical surfaces is the achieved deflection. We then calculated the set of forces and couples needed to provide the difference between the desired deflection and the achieved deflection; these were added to the original forces and couples to provide the set for the second polish.

At this point it is worth noting a subtlety in the iteration procedure. In principle, one might want to fit the interferograms to a Zernike series containing terms higher than fourth order, since the jig

can control terms up to $p^{14}\cos(12\theta)$. In practice, when we fit interferograms with these higher order polynomials, the coefficients were small (~ 0.02 μm) and were attributable to measurement noise, rather than real perturbations in the mirror surface. If one were to interpret these relatively small terms as real and attempt to remove them, one obtains a somewhat surprising result: the forces and couples (and potentially the maximum stress) change radically to produce the slight surface change. This occurs because the mirror is extremely resistant to high spatial frequency deflections; thus large forces are required to introduce or remove relatively small high order displacements. Because of this difficulty, in addition to our expectation that these terms will be small and our observation that these terms were small in practice, we deliberately assumed that all terms above fourth order were zero when the corrective forces and couples were calculated.

The second polish proceeded without difficulty and after about 30 hours the mirror, as determined with the test plate, was estimated to be within about $\lambda/10$ of the test plate sphere. Because the only optical test available to the optician was the undersized test plate, he felt that further improvement would be difficult to achieve.

The mirror was again removed from the stressing jig and the paraboloidal null test proceeded exactly as before. The resulting interferogram is shown in Figure 7. The corresponding Zernike coefficients are listed in Table 1. The surface deviated from the desired paraboloid by 0.16 μm rms.

At this stage the surface differed by a small amount from the desired one. It was now possible to take advantage of two additional

degrees of freedom not yet used in the procedure. In the paraboloidal null tests the mirror was held at a fixed distance from the vertex (R = 35.00 cm) and in a fixed orientation (ϕ = 0) set by the kinematic mount. This distance and angle were measured with respect to the wire pattern which was fixed to invar blocks. By moving the mirror to a slightly different off-axis position (R + δR) and rotating it about its own axis ($\delta\phi$) the mirror can be positioned so that the surface better fits the overall desired paraboloidal surface. Changes in these two degrees of freedom affect the two dominating terms in the expansion of the surface error, astigmatism and coma.

For most applications these small changes can be made in practice by simply optimizing the mirror position in the optical system. For the application to the Ten-Meter-Telescope, the "repositioning" is simply made by defining the position and orientation of the hexagonal cutting needed to make the actual mirror segments after polishing is completed.

Using the definitions of the Zernike coefficients (Table 1) and the equation of a paraboloid (2.1), (2.2), it can be readily shown that the rms deviation between the desired paraboloid and the achieved one is minimized by the following changes in R and ϕ:

$$\delta R = R \frac{8C_{22}\delta C_{22} + 3C_{31}\delta C_{31}}{16C_{22}^2 + 3C_{31}^2}$$

$$\delta\phi = -\frac{8C_{22}\delta C_{2-2} + 3C_{31}\delta C_{3-1}}{16C_{22}^2 + 3C_{31}^2} \qquad (4.1)$$

where the C's and δC's can be found from the data in Table 1. Those coefficients yield $\delta R = +0.73$ mm and $\delta\phi = -6.0 \times 10^{-3}$ radians. This rotation corresponds to an transverse motion of the vertex of -2.1 mm; equivalently a point on the edge of the mirror moves 1 mm. One can also calculate that these changes in the position of the mirror should result in a new set of coefficients with an rms deviation from the new desired section of 0.03 μm. After calculating these motions for the best fitting mirror position we returned to the paraboloidal null test. Using the stage we repositioned the vertex with respect to the mirror as described above. The resulting interferogram is shown in Figure 8. Digitizing the fringe positions and fitting gave the results shown in the final column of Table 1. The fabricated mirror had a measured radius of curvature k = 368.83 cm which differed by 0.03 cm from that desired. The off-axis distance of R = 35.07 cm differed by 0.07 cm from the desired value. The coefficients yield an rms surface error of 0.03 μm.

V. Conclusions

Stressed Mirror Polishing as a technique for making inexpensive, high quality non-axisymmetric mirrors appears to work quite well. The iterative method converges rapidly and in principle should allow mirror fabrication of a quality only limited by the quality of the spherical polish. In practice, limitations in testing procedures will also limit the accuracy in producing the desired mirror. In many applications it may not be necessary to achieve the precisely specified off axis distance and radius of curvature required for a set of matched segments. For these applications the precise and elaborate testing procedure and the limitations it imposed for this demonstration will not be necessary. Slight undesirable edge effects caused by the discrete set of Invar blocks used to apply the forces and couples can be seen in Figure 8. These could be reduced by using more blocks to apply a better approximation to the desired continuous force and couple distributions.

In assessing the general applicability of this technique there are at least four limitations or measures of difficulty which need to be considered: the stress level in the glass, the size of the deflections, the size of the quartic, and the applicability of the theory.

The stress level is important in the sense that if the stress exceeds some level, the mirror may break. Using CerVit, we applied a stress level of 70 kg/cm^2 during grinding and polishing and approached 200 kg/cm^2 during various tests. Since stress is proportional to both thickness and deflection needed, the maximum allowed stress level will limit the applicability of this technique to mirrors that are not extremely thick or severely aspheric. Appropriate stress formulas are

given by LN. It is readily applied to thin mirrors which, unfortunately, require more complex support structures, at least for ground-based uses.

Severely non-spherical surfaces will require large deflections and if the resulting surface quality is expected to be high, the necessary accuracy of the appled forces is large. In our test, the deflections were $\simeq$ 300 times the error in the deflections. By design, our jig is capable of controlling deflections to about 1 part in 10^3. The resulting mirror quality with this system was limited by our spherical polishing and the accuracy of the optical testing. Controlling deflections with a precision better than a part in 10^3 may require a more complex jig than used here. Typically, the deflections will scale as a^2R^2/k^3 so large, severely off-axis mirrors with short radii of curvature are more difficult.

The ability to controllably produce large quartic deflections depends directly on applying completely uniform pressure to the back of the mirror. As mentioned earlier, the difficulties in achieving this can be largely overcome if the pressure distribution is stable in time, since its effects can be compensated for by adjusting the edge forces and couples. Achieving adequate stability becomes increasingly difficult as the quartic deflection increases. Since the needed quartic amplitude varies as $\sim a^4/k^3$, large mirrors with short radii of curvature are more difficult to fabricate with this technique. Since this term is dominantly set by the polished sphere, one could greatly reduce or eliminate the quartic deflection by polishing in an axially symmetric parabola instead of a sphere.

The theory described by LN is only strictly applicable to flat plates, so when the mirror is strongly curved (sagittal depth greater than mirror thickness) the theory may not be appropriate. However, since the technique is iterative, it seems likely that excellent results still can be achieved even though the theory is only approximate.

Since our original motivation was to devise a method of making large off axis segments for the U. C. Ten Meter Telescope, we briefly compare the expected difficulty with these segments to the one we have fabricated. We select the most difficult one for comparison: one with R = 4.85 m, k = 40 m, a = 0.7 m and h = 0.1 m. The maximum induced stress is 13 kg/cm^2, a factor of 4 below that in the test piece, so breakage will not be a problem. The rms deflection is 20 μm or twice what was needed here, so the required accuracy of force application is similar. The quartic deflection, the major expected source of difficulty with this method, is only 0.08 μm, about one fifth of that achieved here, so no difficulty is expected. Finally, the ratio of sagittal depth to mirror thickness is only one third that of our test mirror, so the applicability of the flat plate theory is not in question. As discussed by LN, small variations in the elastic properties of the plate are also not expected to present difficulties.

Acknowledgements

This project was only possible through the support and encouragement of a large number of people. We thank David Saxon, the president of the University of California and Andrew Sessler, the director of the Lawrence Berkeley Laboratory for their financial support and personal encouragement. Owens-Illinois kindly provided samples of CerVit to aid in this test. Tinsley Laboratories was extremely helpful in providing us with their testing and polishing facilities. Julius Meckel of Tinsley was invaluable in teaching us the necessary aspects of optical testing. Roland Wolf of Tinsley polished the sphere and schooled us in the art and science of polishing. Robert Parks of the Optical Sciences Center generously contributed his time and ideas in developing the method for testing the off-axis paraboloid. We greatly appreciate the very successful jig design by Duane Norgren and the aid in its construction from Deborah Haber, Jack Borde, Norm Anderson, Tim Daly, and Mike Long. Special thanks go to Luis Alvarez for his encouragement and support in suggesting very fruitful avenues for the theoretical and practical aspects of this work and for sharing with us his experience with related techniques of mirror bending. Also, this work was supported by the U. S. Department of Energy under Contract W-7405-ENG-48.

REFERENCES

1. Lubliner, J. and Nelson, J. E., "Stressed Mirror Polishing: A Technique for Producing Non-Axisymmetric Mirrors", Lawrence Berkeley Laboratory Report #LBL-9967.

2. Nelson, J., Optical Telescopes of the Future, Conference Proceedings, p. 133 (December, 1977) Geneva 23: ESO c/o CERN 1978 "The Proposed University of California 10 Meter Telescope."

3. Nelson, J. ,Society of Photo-Optical Instrumentation Engineers Proceedings, Volume 172 (January, 1979), "Segmented Mirror Design for a 10-Meter Telescope."

4. Gabor, G., Proceedings of Photo-Optical Instrumentation Engineers Proceedings, Volume 172 (January, 1979), "Position Sensors and Actuators for Figure Control of a Segmented Mirror Telescope".

5. Mast, T.S. and Nelson, J. E., Lawrence Berkeley Laboratory Report # LBL-8621 (March, 1979) " Figure Control for a Segmented Telescope Mirror".

6. Born, M. and Wolf, E., Principles of Optics, 4th edition Pergamon Press (1970), p. 466.

7. Timoshenko, S. and Woinowsky-Krieger, S., Theory of Plates and Shells, 2nd edition, McGraw-Hill, 1959.

FIGURE CAPTIONS

1. Diagram defining the global (X,Y,Z) and local coordinates (x,y,z = ρ,θ,z) of the mirror segment on the paraboloid.

2. Zernike coefficients describing the surface of an off-axis section of a paraboloid as a function of off-axis distance R. The paraboloid has a radius of curvature k = 368.80 cm and the segment radius is a = 17.94 cm. The desired surface for the fabricated mirror (R = 35.00 cm) is dominated by astigmatism and coma.

3. Schematic showing the mirror blank, an Invar block, a radial arm, and the lever and weight system used to apply forces F_1 and F_2. Twenty-four such assemblies produced the shear forces and moments to stress the mirror.

4. Schematic diagram showing the geometry of the paraboloidal null test. The focus of the Twyman-Green interferometer is located at the vertex of the global paraboloid. The mirror section under test is fixed 35.00 cm from the vertex.

5. Interferogram from a spherical null test of the spherical mirror under stress before polishing. The applied forces and couples and the coefficients describing the surface are listed in Tables 1 and 2. The surface is an "anti-parabola" dominated by 19.4 μm of astigmatism (saddle) and 6.6 μm of coma (internal extremum). The fringes are half wave, 632.8 nm/2. The contour plot of the surface is generated from the coefficients from the fourth order fit.

6. Interferogram from the paraboloidal null test after the first polish. The fringes (quarter wave = 632.8 nm/4) show the difference between the desired and achieved paraboloidal sections. This error surface is dominated by focus and astigmatism and its rms amplitude is 0.55 μm. The contour plot of the surface is generated from the coefficients from the fourth order fit.

7. Interferogram from the paraboloidal null test after the second polish. The fringes (quarter wave = 632.8 nm/4) show the difference between the desired and achieved paraboloidal sections. The error surface is dominated by astigmatism and the rms amplitude is 0.16 μm. The contour plot of the surface is generated from the coefficients from the fourth order fit.

8. Interferogram from the paraboloidal null test with the mirror in the best fit position. The fringes (quarter wave = 632.8 nm/4) show the difference between the desired and achieved surfaces. The rms error is 0.03 μm. The contour plot of the surface is generated from the coefficients from the fourth order fit.

APPENDIX 1

The Effects of Support Pad Non-Uniformities

The elastic deformation of a plate under external loads can be calculated using thin plate theory as described by Timoshenko[7] or by LN. To describe the deformations induced by the pad and jig we wish to solve the equation

$$D \nabla^4 \omega = q \qquad (A.1)$$

D, the flexural rigidity (see Timoshenko[7] or LN) is a constant subject to the boundary conditions that the shear force and couple are specified at the edge of the plate and ω and q are the displacement and applied back pressures respectively. These constraints are described by LN in equations A.3 and A.6.

We are interested here in the plate deformations due to non-uniform pad pressure. Since the equation is linear, it is sufficient to solve problem for a free edge (shear force and couple both vanish at the edge) and add this solution to the solution found with a uniform pad and the boundary conditions needed to produce the desired deformations (solved in LN).

The desired quartic deformation is achieved with a uniform pad pressure. We assume that the non-uniformities in the pad pressure will be proportional to the desired uniform pressure. Thus the deformations caused by pad non-uniformities will be proportional to the size of the desired quartic term.

With a uniform pad pressure, q_{00}, the resulting deflection is given by

$$\omega = -\frac{q_{00}}{32D}\,\frac{3+\nu}{1+\nu}\,\rho^2 + \frac{q_{00}}{64D}\,\rho^4 \quad . \qquad \text{(A.2)}$$

where we have assumed the plate has a unit radius, ν is Poisson's ratio and ρ is the radial variable.

It is convenient to describe the pressure distribution of a non-uniform pad with an expansion in orthogonal functions, the Zernike polynomials. Thus we can write the pad pressure as

$$q(\rho,\theta) = \sum_{n=0}^{\infty} \sum_{m=-n}^{n} q_{nm}\, Z_{nm}(\rho,\theta) \qquad n-m \text{ even} \quad \text{(A.3)}$$

We simplify this somewhat by including only the cos $m\theta$ terms ($m \geq 0$) and only the lowest order terms. Explicitly we assume only q_{11}, q_{20}, q_{22}, q_{31} are non zero. Since the boundary conditions require that the mirror experience no net turning moment, $q_{11} = 0$. The uniform pressure, q_{00}, is zero since its effects are accounted for in the originally posed problem.

The resulting deflections are also conveniently described by a series expansion in orthogonal functions:

$$\omega(\rho,\theta) = \sum_{n=0}^{\infty} \sum_{m=-n}^{n} C_{nm}\, Z_{nm}(\rho,\theta) \qquad n-m \text{ even} \quad \text{(A.4)}$$

Inserting A.3 and A.4 into equation A.1 and applying the boundary conditions yields

$$C_{20} = \frac{7+2\nu}{480(1+\nu)}\,\frac{q_{20}}{D}$$

$$C_{22} = \frac{303+18\nu-\nu^2}{3840(1-\nu)(3+\nu)}\,\frac{q_{22}}{D}$$

$$C_{31} = \frac{41 + 7\nu}{5760(3 + \nu)} \frac{q_{31}}{D}$$

$$C_{40} = -\frac{1}{576} \frac{q_{20}}{D}$$

$$C_{42} = -\frac{1}{2304} \frac{15 + \nu}{3 + \nu} \frac{q_{22}}{D} \qquad \text{(A.5)}$$

$$C_{51} = -\frac{1}{1680} \frac{q_{31}}{D}$$

$$C_{60} = \frac{1}{5760} \frac{q_{20}}{D}$$

$$C_{62} = \frac{1}{5760} \frac{q_{22}}{D}$$

$$C_{71} = \frac{1}{13440} \frac{q_{31}}{D}$$

It now convenient to describe the change in the C_{ij}'s caused by the pad non-uniformities in terms of the ratio of non-uniform to uniform pressures. Defining

$$\varepsilon_{ij} = \frac{q_{ij}}{q_{00}} \quad \text{and} \quad r_{ij} = \frac{C_{ij}}{C_{40}^{0}} \qquad \text{(A.6)}$$

where C_{40} is the quartic deflection from a uniform pad ($= q_{00}/384D$), and assuming $\nu = 0.25$, we find

$$r_{20} = 4.80\ \varepsilon_{20} \qquad r_{51} = -0.23\ \varepsilon_{31}$$

$$r_{22} = 12.61\ \varepsilon_{22} \qquad r_{60} = 0.067\ \varepsilon_{20}$$

$$r_{31} = 0.88\ \varepsilon_{31} \qquad r_{62} = 0.067\ \varepsilon_{22} \qquad \text{(A.7)}$$

$$r_{40} = -0.67\ \varepsilon_{20} \qquad r_{71} = 0.029\ \varepsilon_{31}$$

$$r_{42} = -0.78\ \varepsilon_{22}$$

We see from A.7 that the astigmatic deflection is the most easily induced aberration, followed by focus. As one might expect, higher order deflections are substantially more difficult to create. These results are qualitatively confirmed by our tests with a variety of pads where astigmatism was the dominant aberration induced by pad non-uniformity.

TABLE 1

					Zernike Coefficients (μm)				
n	m	$Z_{nm}(\rho,\theta)$	Cylindrical Monomial Coefficient Relationship	Weight	Desired Deflections	Desired Parabola	First* Polish	Second* Polish	Measured Residuals from Best Fitting Paraboloid
0	0	1	$C_{00} = \alpha_{00} + \frac{\alpha_{20}}{2} + \frac{\alpha_{40}}{3} + \cdots$	1					
1	-1	$\rho\sin\theta$	$C_{1-1} = \alpha_{1-1} + \frac{2}{3}\alpha_{3-1} + \cdots$	$\frac{1}{4}$		k=368.80 cm R= 35.00 cm ϕ= 0.0	k=368.68 cm R= 35.79 cm ϕ= 0.0043	k=368.83 cm R= 35.07 cm ϕ= -0.0060	
1	1	$\rho\cos\theta$	$C_{11} = \alpha_{11} + \frac{2}{3}\alpha_{31} + \cdots$	$\frac{1}{4}$					
2	-2	$\rho^2\sin2\theta$	$C_{2-2} = \alpha_{2-2} + \frac{3}{4}\alpha_{4-2} + \cdots$	$\frac{1}{6}$	0.00	0.00	-0.15	0.24	0.02
2	0	$2\rho^2 - 1$	$C_{20} = \frac{\alpha_{20}}{2} + \frac{\alpha_{40}}{2} + \cdots$	$\frac{1}{3}$	-8.93	2161.88	2162.59	2161.68	0.00
2	2	$\rho^2\cos2\theta$	$C_{22} = \alpha_{22} + \frac{3}{4}\alpha_{42} + \cdots$	$\frac{1}{6}$	19.34	-19.34	-20.21	-19.42	-0.02
3	-3	$\rho^3\sin3\theta$	$C_{3-3} = \alpha_{3-3} + \cdots$	$\frac{1}{8}$	0.00	0.00	0.02	0.02	0.01
3	-1	$(3\rho^3 - 2\rho)\sin\theta$	$C_{3-1} = \frac{\alpha_{3-1}}{3} + \cdots$	$\frac{1}{8}$	0.00	0.00	-0.16	-0.01	-0.05
3	1	$(3\rho^3 - 2\rho)\sin\theta$	$C_{31} = \frac{\alpha_{31}}{3} + \cdots$	$\frac{1}{8}$	6.55	-6.55	-6.71	-6.55	0.01
3	3	$\rho^3\cos3\theta$	$C_{33} = \alpha_{33} + \cdots$	$\frac{1}{8}$	-0.04	0.04	0.00	0.00	-0.04
4	-4	$\rho^4\sin4\theta$	$C_{4-4} = \alpha_{4-4} + \cdots$	$\frac{1}{10}$	0.00	0.00	0.02	0.02	0.03
4	-2	$(4\rho^4 - 3\rho^2)\sin2\theta$	$C_{4-2} = \frac{\alpha_{4-2}}{4} + \cdots$	$\frac{1}{10}$	0.00	0.00	0.02	0.00	0.00
4	0	$6\rho^4 - 6\rho^2 + 1$	$C_{40} = \frac{\alpha_{40}}{6} + \cdots$	$\frac{1}{5}$	0.40	0.01	-0.11	0.04	0.03
4	2	$(4\rho^4 - 3\rho^2)\cos2\theta$	$C_{42} = \frac{\alpha_{42}}{4} + \cdots$	$\frac{1}{10}$	-0.01	0.01	-0.07	0.02	0.00
4	4	$\rho^4\cos4\theta$	$C_{44} = \alpha_{44} + \cdots$	$\frac{1}{10}$	0.00	0.00	-0.01	0.04	0.05
						$(Z - Z_{desired})_{rms}$	0.55	0.16	
						$(Z - Z_{best})_{rms}$	0.08	0.03	

*The values of k, R, and ϕ given are the best fitting values determined from the tabulated Zernike coefficients.

TABLE 2

		First Polish		Second Polish	
Angle	Lever No.	Force, kg	Couple, kg-cm	Force, kg	Couple, kg-cm
15°	1	-16.78	260.38	-15.75	246.56
30°	2	-17.73	213.92	-16.76	204.70
45°	3	-18.73	144.59	-17.74	141.79
60°	4	-19.07	62.68	-18.13	65.98
75°	5	-18.06	-20.54	-17.28	-13.00
90°	6	-15.29	-95.13	-14.62	-85.56
105°	7	-10.73	-154.32	-9.98	-144.65
120°	8	-4.86	-195.48	-3.88	-187.35
135°	9	1.46	-219.94	2.58	-214.84
150°	10	7.11	-231.82	8.13	-230.66
165°	11	11.03	-236.22	11.73	-238.43
180°	12	12.43	-237.17	12.84	-240.42
195°	13	11.03	-236.22	11.39	-237.21
210°	14	7.11	-231.82	7.65	-228.03
225°	15	1.46	-219.94	2.16	-211.07
240°	16	-4.86	-195.48	-4.19	-183.51
255°	17	-10.73	-154.32	-10.26	-142.20
270°	18	-15.29	-95.13	-14.92	-85.27
285°	19	-18.06	-20.54	-17.48	-14.22
300°	20	-19.07	62.68	-17.98	64.86
315°	21	-18.73	144.59	-17.14	142.06
330°	22	-17.73	213.92	-15.93	206.20
345°	23	-16.78	260.38	-15.14	247.96
360°	24	-16.40	276.73	-15.11	261.82

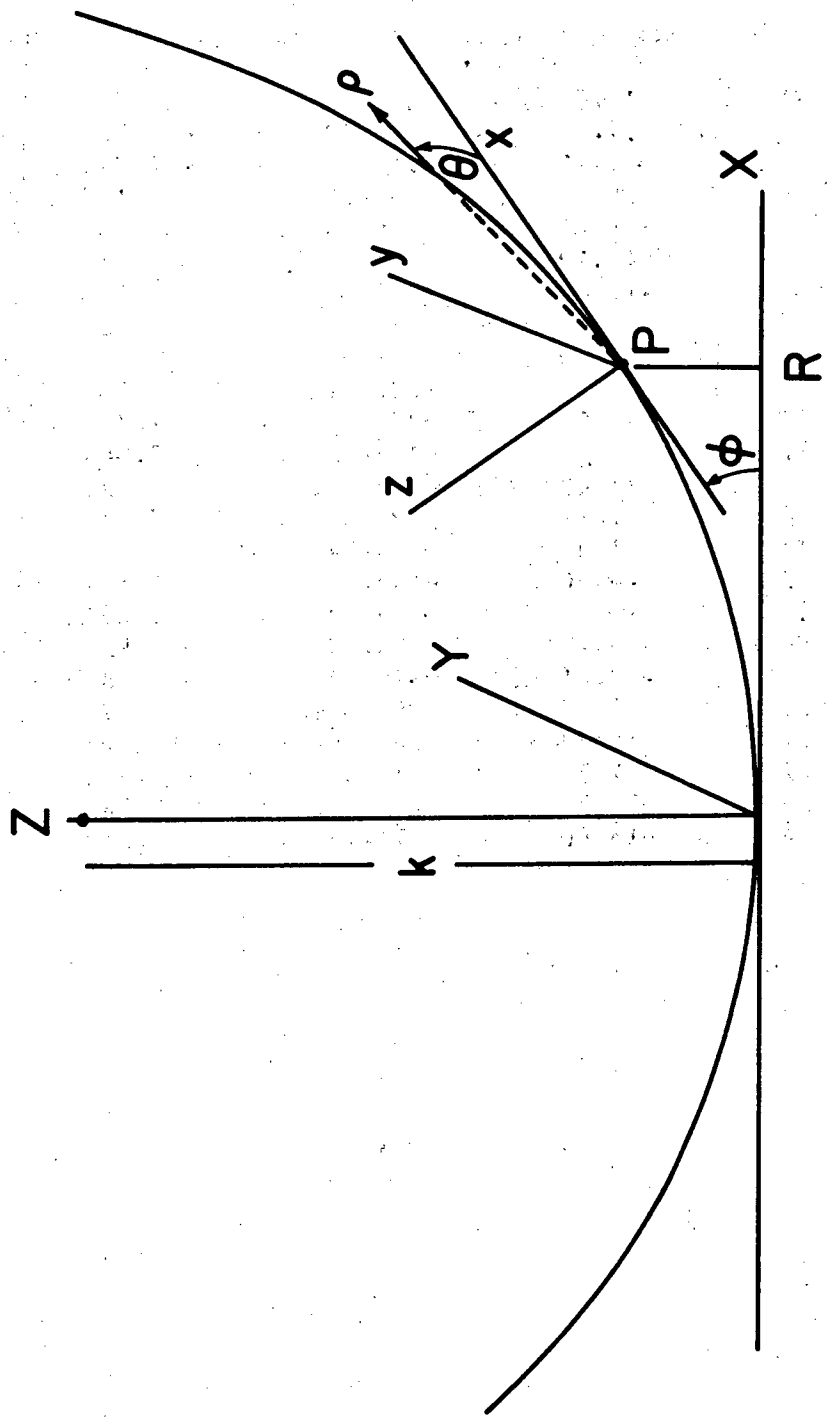

XBL 7912-13613

Figure 1

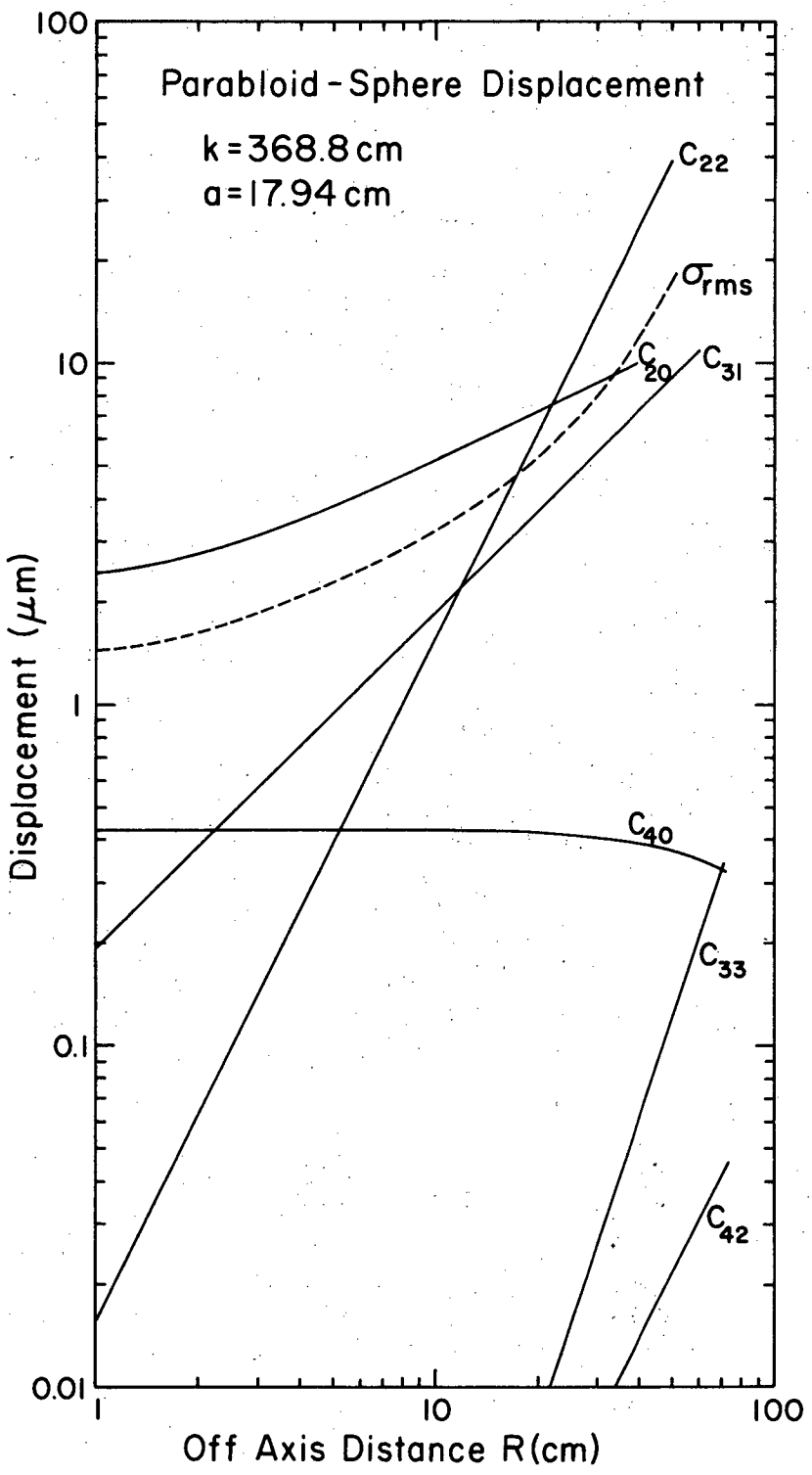
Parabloid - Sphere Displacement
k = 368.8 cm
a = 17.94 cm
C22
σrms
C20
C31
C40
C33
C42
100
10
1
0.1
0.01
Displacement (μm)
1
10
100
Off Axis Distance R(cm)
XBL 7912-13609

Figure 2

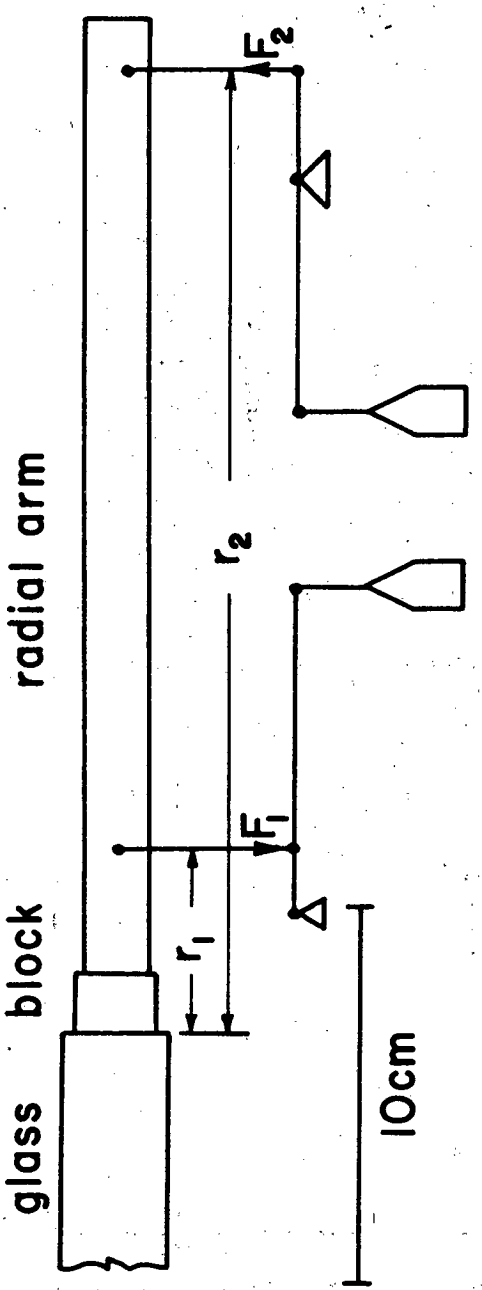

XBL 7912-13612

Figure 3

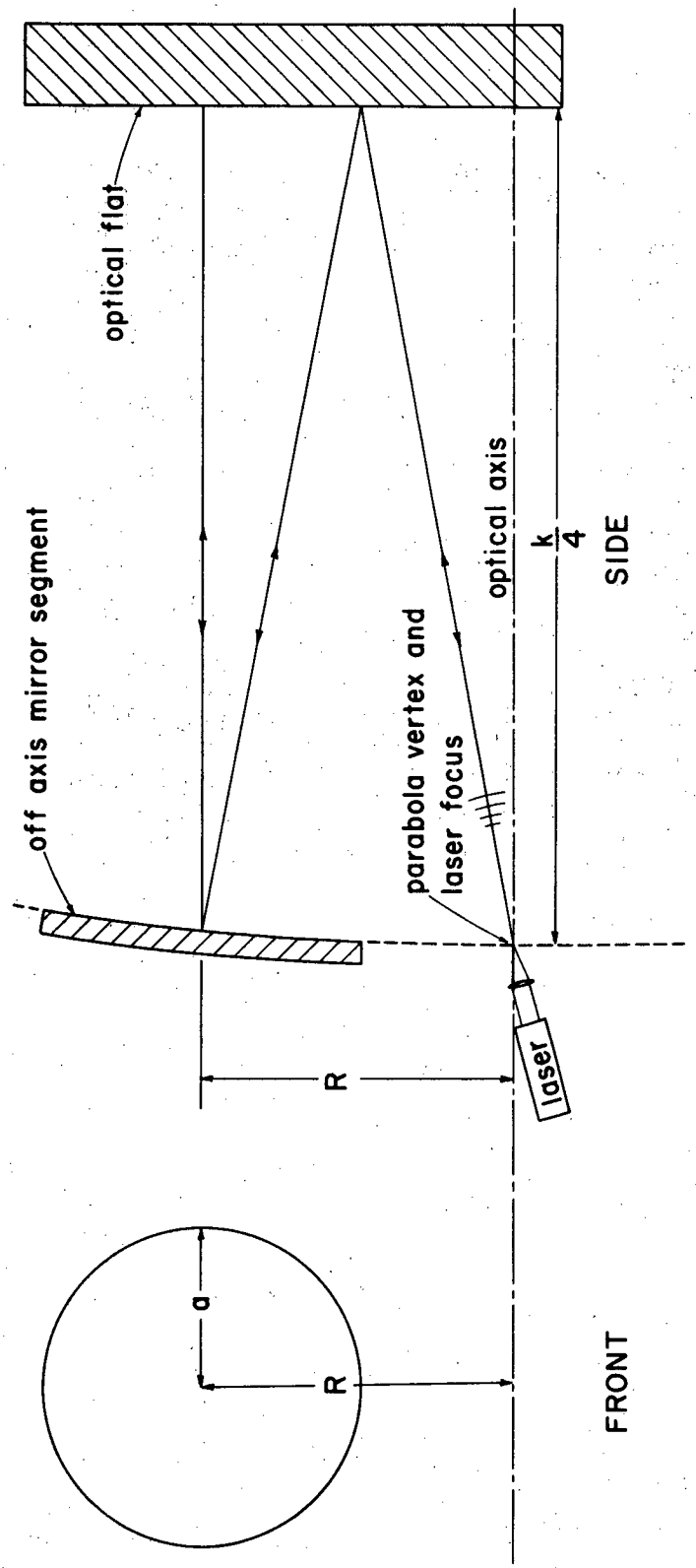
optical flat
off axis mirror segment
parabola vertex and
laser focus
optical axis
k/4
SIDE
R
laser
a
R
FRONT
XBL 7912-13607

Figure 4

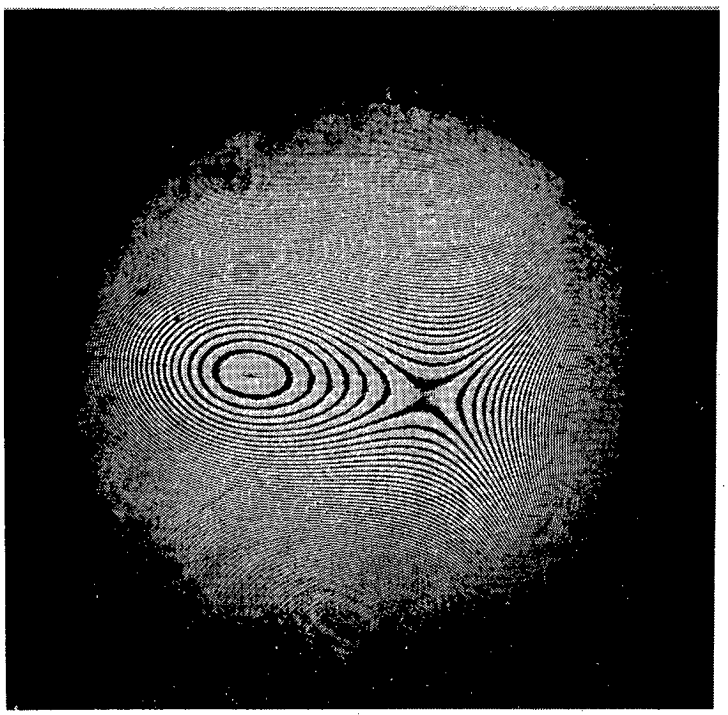

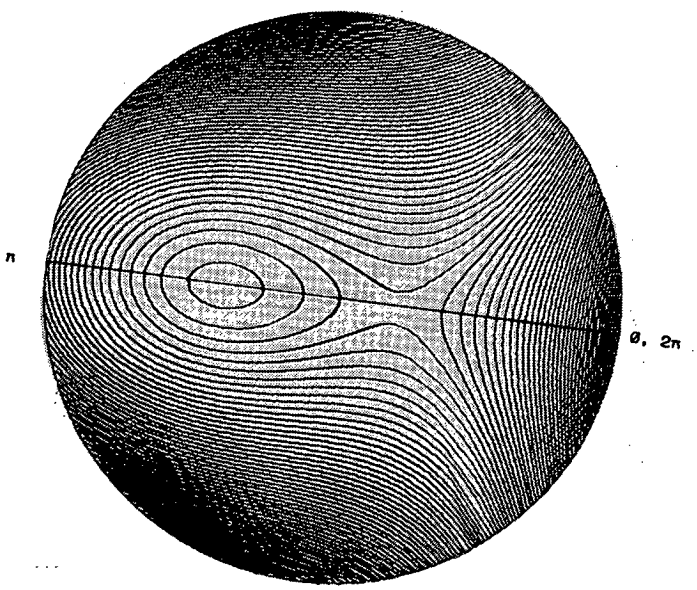

XBB 795-7438A

Figure 5

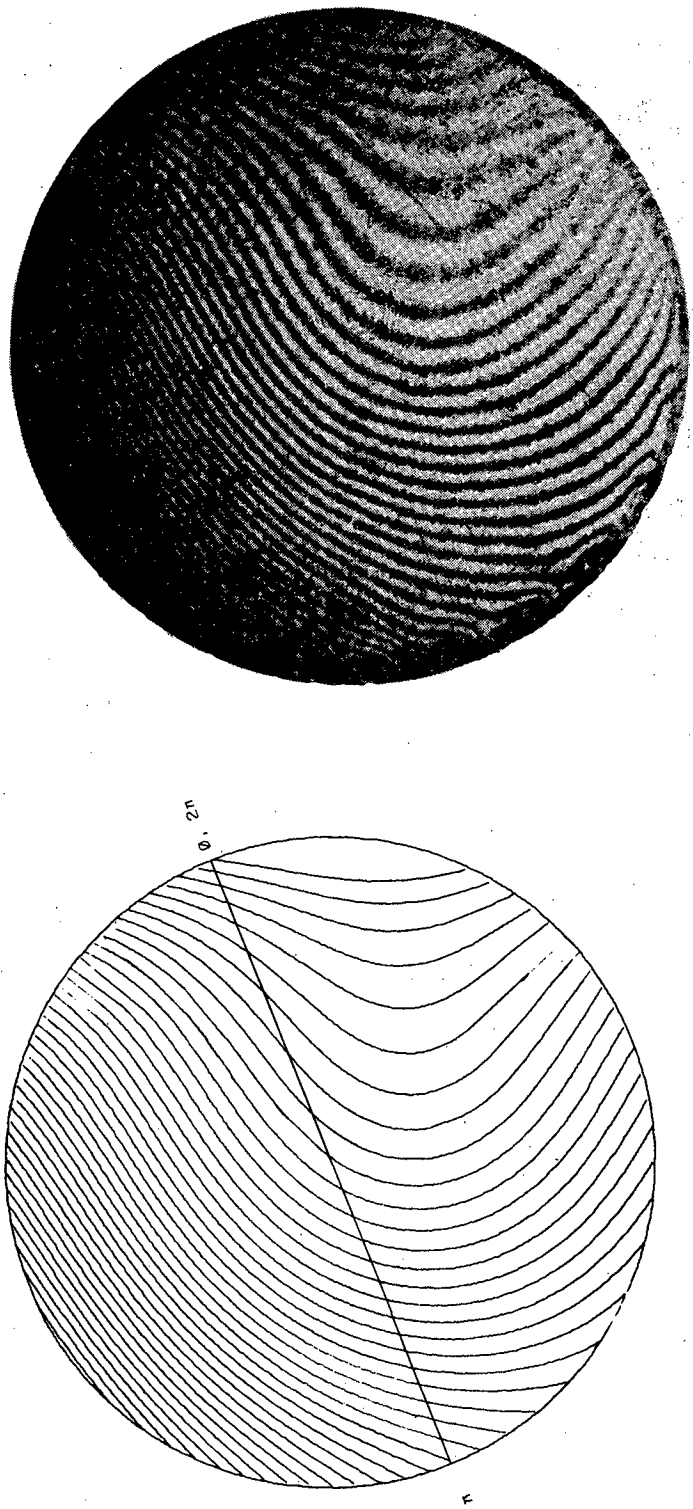

XBB 790-14522A

Figure 6

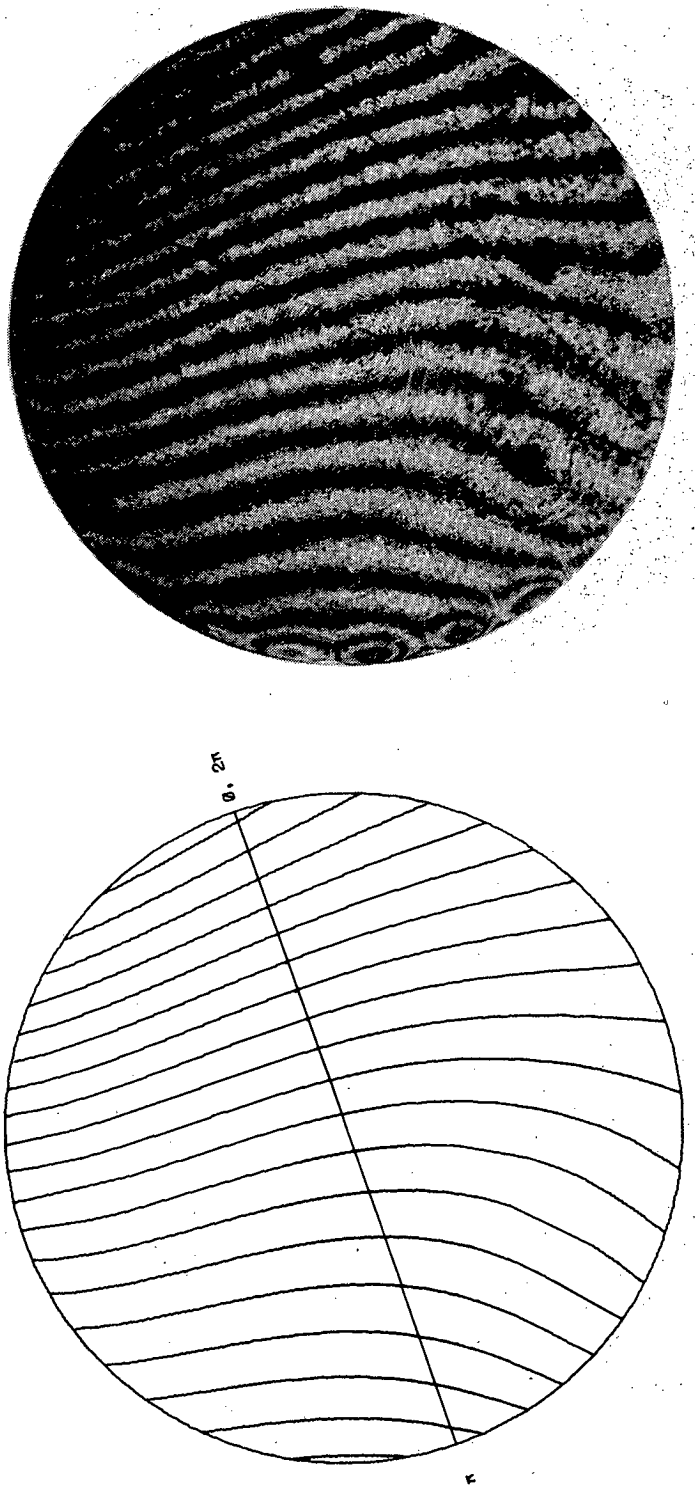

XBB 790-14523A

Figure 7

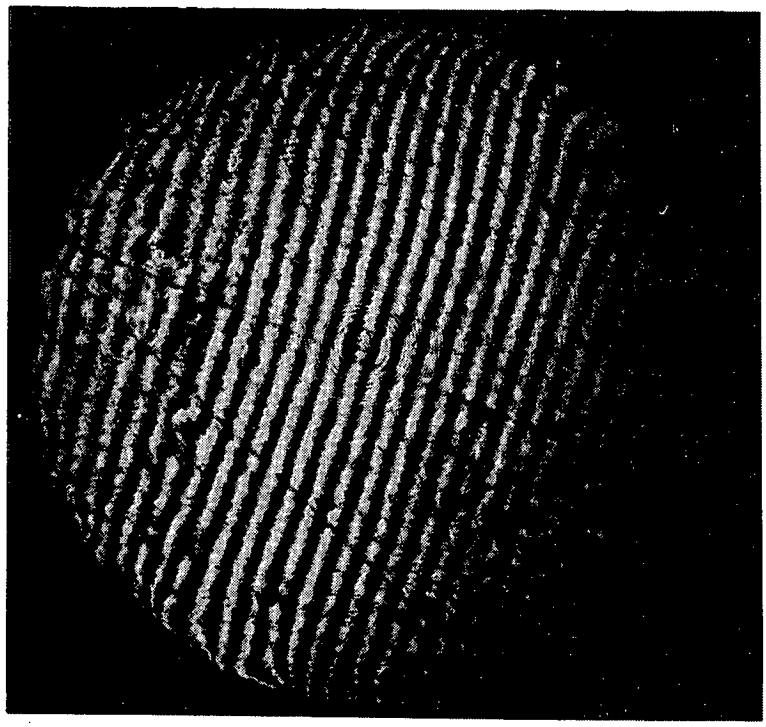

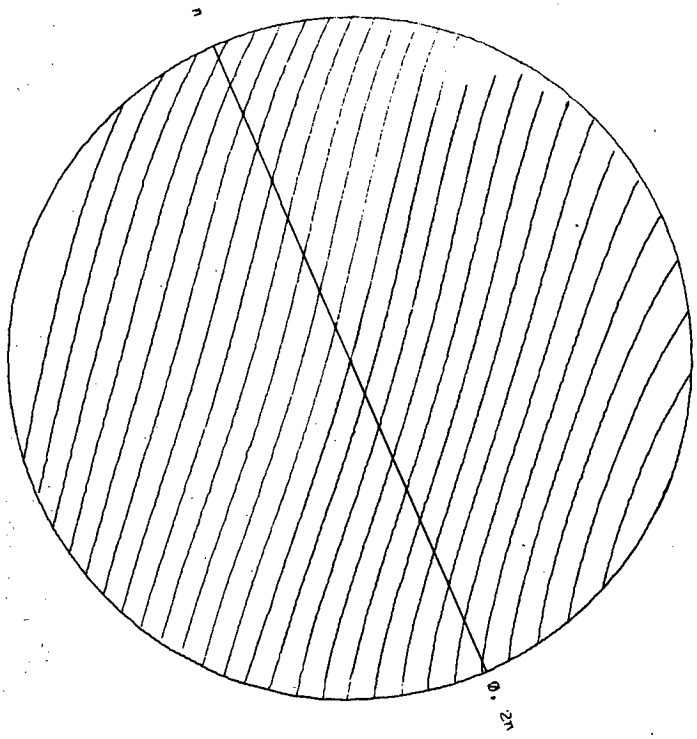

XBB 797-9804A

Figure 8

TECHNICAL INFORMATION DEPARTMENT
LAWRENCE BERKELEY LABORATORY
UNIVERSITY OF CALIFORNIA
BERKELEY, CALIFORNIA 94720